

Full length article

Theoretical analysis of the influence of electron beam parameters on the harmonic powers in free electron lasers

K. Zhukovsky*, I. Fedorov, N. Gubina

Department of Theoretical Physics, Faculty of Physics, M.V.Lomonosov Moscow State University, Moscow 119991, Russia

ARTICLE INFO

Keywords:

Radiation
Harmonics
Undulator
Free electron laser
Electron beam

ABSTRACT

We theoretically analyse the influence of the electron beam parameters on the radiation in free electron lasers (FELs). We consider three FEL installations, SPARC, LEUTL and SwissFEL, where several experiments with different values of the beam emittance, energy spread and current were conducted and documented in details. Based on the available data and on our analytical approach to the FEL harmonic power computation, we distinguish the key factors, affecting the harmonic generation, and compare our theoretical results with the available experimental data. Alternative theoretical approaches were also employed for the harmonic power estimation. At the reviewed installations and experiments the variation of the emittance, energy spread and electron current occurred; we model these experiments with account for all variations, and analyze and compare the results with each other for different sets of parameters; we compare the results with the available experimental data and measurements. We demonstrate as the emittance, the energy spread and the beam current density values interplay in their influence on the radiation characteristics of a single pass FEL and we show as individual variations of these parameters can mutually compensate each others influence to some degree.

1. Introduction

The undulator radiation (UR) was discovered by Motz [1], who followed the idea of Ginzburg [2] about the radiation from electrons in a spatially periodic magnetic field. The coherent UR from electrons in undulators was hypothesized by Ginzburg and discovered by Madey [3], who developed a rigorous theory behind the interactions of electrons and radiation in an undulator. The force of interaction in the undulator groups electrons in microbunches along the undulator length at the wavelength of the UR. This effect is used in free electron lasers (FELs), where undulators generate coherent radiation in wide range of wavelengths up to hard X-rays. In this band quasi-monoenergetic beams with very low emittance and high current are needed for efficient grouping of electrons in a single pass FEL. Theory and applications of FEL radiation are broadly discussed in literature [4–14] et al. FEL is based on that radiation travels slightly faster than electrons in an undulator and the lag between the radiation and the electrons is just enough for the Lorenz force to be always directed towards the nodes of the radiation wave in the undulator. The electrons are bunched at the radiation wavelength; bunching at harmonic wavelengths is weaker and very sensitive to the losses, associated with the beam divergence, energy spread, diffraction

etc. Thus, generation of FEL harmonics imposes tight requirements on the whole installation.

The resonances of the UR are at the following wavelengths:

$$\lambda_n = \frac{\lambda_u}{2n\gamma^2} \left(1 + \frac{k_{eff}^2}{2} + (\gamma\theta)^2 \right) \quad (1)$$

where n is the number of UR harmonic, θ is the angle off the axis, $k_{eff}^2 = k^2\varpi$ is the effective undulator parameter, and $k = H_0\lambda_u e/2\pi mc^2$ is the deflection parameter, while $\varpi = 1 + (d/h)^2$ describes the effect of the field harmonic, such as $h = 1$ in a helical undulator, H_0 is the magnetic field amplitude on the axis, d is the relative amplitude of the field harmonic, e is the electron charge, λ_u is the undulator period; the value of the undulator deflection parameter is easy to compute as follows: $k \approx 0.9337H_0[T]\lambda_u[cm]$. In modern FELs the undulator parameter values are $k \sim 2-3$ and for the visible range of radiation the electron energy is $E \sim 100-200$ MeV, while for the X-ray radiation the beam energy is $\sim 5-15$ GeV. The on-axis spontaneous radiation spectrum from a planar undulator ideally consists of odd harmonics. Even harmonics are radiated mainly off the axis. On-axis even harmonic radiation occurs in beams of finite size. In real installations not only the beams have finite

* Corresponding author.

E-mail address: zhukovsk@physics.msu.ru (K. Zhukovsky).

size and emittance, but also the energy spread is non zero and this affects high harmonics much more than the fundamental. Harmonic content of a FEL is much narrower than for the spontaneous UR. FEL radiation requires the conditions for the emittance $\varepsilon_{x,y} \leq \lambda_0/4\pi$ and for the energy spread $\sigma_e \leq \rho/2$ fulfilled at least weakly (see [4–10]); they are not always strictly satisfied in practice, but in weaker conditions, $\varepsilon_{x,y} \sim \lambda_0/4\pi$ and $\sigma_e \approx \rho_n$, the generation may be possible. Typical single pass FEL spectrum consists of the fundamental and the third harmonic, whose power is 1–2 % or less; other harmonics, if present, are usually one order of magnitude weaker [15–19]. Exact solution of equations for interactions of charges and radiation, energy exchange and beam dynamics, is not possible analytically. This engineering problem can be addressed numerically (see multiple examples in [20–22]). However, numerical modelling of a FEL requires prepared personnel, good computational facilities and the software installed and working. Numerical modelling usually gives accuracy of one order of magnitude for the fundamental tone and one–two orders of magnitude discrepancy for the harmonics. In reality there are always errors of magnetization, assembly etc., so that an order of magnitude is a fairly good accuracy, considering logarithmic scale of the exponential power growth in a FEL. Alternatively to numerical modelling, simple phenomenological analytical descriptions exist and some of them give consistently good results. Based on early studies in [23–26], we developed such formalism, which involves generalized forms of Bessel and Airy functions and phenomenological description of FEL harmonic power evolution in a FEL. Calibrated with all large data for major FELs from visible band to X-rays, the analytical description consistently gives predictions within the range of measurements for existing FELs and agrees with numerical simulations and models as demonstrated in [20,21,27–29]. Our analytical approach traces the effects of beam and undulator parameters on the FEL radiation. Thus it becomes possible to explain and predict the behaviours of harmonics and effect of the installation parameters on them.

In what follows we will study the FEL radiation at SPARC, LEUTL and SwissFEL and compare the results with existing data. We will explore the reasons for the measured harmonic content and also explain the effect of the variation of the beam parameters on the harmonic behaviours in each of the considered FELs.

2. Analytical formalism for the estimates of the effect of beam parameters on the radiation

The analytical expression for the UR intensity from a single electron is well known and it reads as follows:

$$\frac{d^2 I}{d\omega d\Omega} \cong \frac{e^2 \gamma^2 N^2 k^2}{c \left(1 + \left(k_{\text{eff}}^2/2\right) + (\gamma\theta)^2\right)} \sum_{n=-\infty}^{\infty} n^2 \text{sinc}^2\left(\frac{\nu_n}{2}\right) \left(f_{n,x}^2 + f_{n,y}^2\right) \quad (2)$$

where $\nu_n = 2\pi n N ((\omega/\omega_n) - 1)$ is the detuning parameter, $\omega_n = 2\pi c/\lambda_n$ are the UR resonances; $f_{n,x,y}$ are the Bessel coefficients for the x- and y-polarizations. The Bessel coefficients f_n strongly depend on the undu-

single period planar undulator, where field harmonics are weak, their effect on the UR harmonics can be largely neglected. In this case the Bessel coefficients $f_{n,x,y}$ in (2) reduce to relatively simple expressions [23,25,26,30] et al.:

$$\begin{aligned} f_{n,x} &= \sum_p \tilde{J}_p \left| \left(J_{n+1}^m + J_{n-1}^m \right) + \frac{2}{k} \gamma \theta \cos \varphi J_n^m \right|, f_{n,y} \\ &= \sum_p \left(\tilde{J}_p \left| \frac{2}{k} \gamma \theta \sin \varphi J_n^m \right| + J_n^m \frac{\sqrt{2} \pi y_0}{\lambda_u} \left(\tilde{J}_{p+1} - \tilde{J}_{p-1} \right) \right), \end{aligned} \quad (3)$$

involving the Bessel functions J_n^m and \tilde{J}_p , and account for the finite beam size y_0 and for the off-axis effects in the angle θ . The integral form of the Bessel functions for a planar undulator is the following:

$$\begin{aligned} J_n^m &\equiv J_n^m(\zeta, \xi) \cong \int_{-\pi}^{\pi} \frac{d\alpha}{2\pi} \exp[i(n\alpha + m\zeta \sin \alpha + m\xi \sin(2\alpha))], \tilde{J}_p \\ &\equiv J_p^1(-\kappa, -\eta) \end{aligned} \quad (4)$$

where the arguments of the generalized Bessel functions J_i^j read as follows:

$$\zeta = \theta \cos \varphi \frac{\lambda_u k}{n \lambda_n \gamma}, \quad \xi = \frac{\lambda_u k^2}{8 n \lambda_n \gamma^2}, \quad \kappa = \frac{4\pi \theta y_0 \gamma^2}{\lambda_u (1 + (k^2/2))}, \quad \eta = \frac{\pi^2 \gamma y_0^2 k}{\sqrt{2} \lambda_u^2 (1 + (k^2/2))} \quad (5)$$

Betatron oscillations in a finite-sized beam split each harmonic with frequency $\omega_n = 2\pi c/\lambda_n$ into betatron radiation harmonics, distant from each other by the frequency $\omega_\beta \cong \frac{\omega_n k}{\sqrt{2n\gamma}}$ (see, for example, [39]). For relativistic beams $\omega_\beta \ll \omega_n/\gamma$, and $\omega_\beta \ll \omega_n$ since $\gamma \gg 1$; each radiation line is then split into betatron harmonics close to each other. Bessel coefficients and Bessel functions are used for the stimulated radiation analysis too.

For the spontaneous UR the account for the electron energy spread σ_e in a beam is usually done by the following convolution:

$$\frac{d^2 I(\sigma_e)}{d\omega d\Omega} = \int_{-\infty}^{+\infty} d^2 I(\nu_n + 4\pi n N \varepsilon) e^{-\varepsilon^2/2\sigma_e^2} d\varepsilon / d\omega d\Omega \sqrt{2\pi} \sigma_e \quad (6)$$

where N is the number of undulator periods. Angular effects, including the angles, induced by dipole magnetic fields, were analytically studied in [40–43]. A complicated expression with generalized Airy-type functions arises in this case. Proper convolution, which accounts for the energy spread, angular effects and the dipole fields, is cumbersome. Other than periodic magnetic fields are usually screened out or compensated upon calculation of field integrals in undulators. Considering the energy spread and angular affects, for example, due to large emittance, only the argument $\sim \tau$ remains in the Airy-type function $S(\nu_n, \eta, \beta) \equiv \int_0^1 e^{i(\nu_n \tau + \eta \tau^2 + \beta \tau^3)} d\tau$ (see [40–44]). The proper convolution, describing the degradation of the UR line due to the homogeneous and inhomogeneous spread, reduces to some simpler form [40–44]:

$$\begin{aligned} \frac{d^2 I(\theta, \sigma_e)}{d\omega d\Omega} &\cong \frac{e^2 \gamma^2 N^2 k^2}{c \left(1 + \left(k_{\text{eff}}^2/2\right) + \gamma^2 \theta^2\right)} \times \\ &\sum_{n=-\infty}^{\infty} n^2 \left(f_{n,x}^2 + f_{n,y}^2\right) \int_{-\infty}^{\infty} \frac{d\varepsilon e^{-\varepsilon^2/2\sigma_e^2}}{\sqrt{2\pi} \sigma_e} \left(\int_0^1 \exp \left\{ i\tau \left(\nu_n + 4\pi n N \varepsilon + \frac{2\pi n N (\gamma\theta)^2}{1 + \left(k_{\text{eff}}^2/2\right) + (\gamma\theta)^2} \right) \right\} d\tau \right)^2. \end{aligned} \quad (7)$$

lator type and its parameters; account for field harmonics yields cumbersome integrals and the result for multiple field harmonics in both directions can be very complicated (see for example, [28–38]). For a

Numerical integration over the angles with their proper distribution

in the beam, for example, Gaussian, can be lengthy on certain machines. The effective values for the divergences can be used instead for a simple estimate; the result appears in good agreement with numerical models, such as SPECTRA. The difference between the results from (7) and (6) is minor if the emittance of the beam is moderate. Our computer experiments show that for $\beta \sim 1-2$ m, the emittances up to few mm \times mrad can be well treated with a simple convolution. Only for large emittances, such as that of LEUTL, the convolution (7) is needed.

Phenomenological description of FEL harmonics evolution along undulators was presented in a number of our recent publications [23–26,28–38], it develops the earlier version of the analytical description in [45,46]. Omitting all details we just give some essential equations for the harmonic power computation. Fundamental role in FEL physics plays the Pierce parameter $\rho = (\lambda_u g_0)/4\pi$ [4–7], related to the FEL signal gain g_0 . The Pierce parameter is determined by the undulator parameters: deflection parameter k_{eff} , period λ_u , the Bessel coefficients $f_{n,x,y}$, and the beam properties: the relativistic factor γ , current I_0 and beam cross section Σ , as follows (see [4–10]):

$$\begin{aligned} P_{n,0} &\cong c_n b_n^2 P_{n,F}, \quad \tilde{P}_{n,0} \cong d_n b_n^2 P_{n,F} |_{\eta \rightarrow \tilde{\eta}}, \quad \tilde{\eta} = \eta |_{\phi \rightarrow \tilde{\phi}}, \quad \tilde{\Phi} = \Phi |_{\mu \rightarrow \tilde{\mu}}, \quad \tilde{\mu} = n\mu, \quad b_n^2 = \left(P_{1,0} / P_e \tilde{\rho}_1 \right)^n, \\ \tilde{P}_{n,F} &= P_{n,F} |_{\eta \rightarrow \tilde{\eta}}, \quad \bar{P}_{n,F} \cong \frac{P_{n,F} \left(1 + 0.3 \left(n(z - L_s) / 1.3 L_g \right) \right) - 0.5 \tilde{P}_{n,F}}{1.3}, \quad c_n = \{1, 1.3, 2, 5, 10\}, \quad d_n = \{1, 3, 8, 40, 120\} \end{aligned} \quad (13)$$

$$\rho_n = \frac{1}{2\gamma} \left(\frac{I_0 / \Sigma}{4\pi i} \right)^{1/3} (\lambda_u k_{eff} |f_n|)^{2/3} \quad (8)$$

where $i = 4\pi\epsilon_0 mc^3 / e$ is the Alfvén current dimensional constant, $i \cong 1.7045 \times 10^4$ [A] in Amperes. The beam diffraction, energy spread, emittance etc. reduce the value of the Pierce parameter, which is reciprocal the gain length $L_{g0} = 1/\sqrt{3}g_0$. Phenomenological approximation of Ming Xie [47,48] accurately accounts for all kinds of losses and gives proper correction Λ to the gain length: $L_g = L_{g0}(1 + \Lambda)$, where Λ contains nineteen coefficients in the polynomial form. Instead of that we use somewhat simpler formulation. The correction to the Pierce parameter ρ_n [45,46], which accounts for the diffraction, reads as follows:

$$\rho_n \rightarrow \tilde{\rho}_n = \rho_n / \kappa, \quad \kappa = \sqrt[3]{1 + \frac{\lambda_u \lambda_n}{16\pi \rho_n \Sigma}} \quad (9)$$

This correction to the Pierce parameter affects the gain length $L_{n,g}^0 \cong \lambda_u / (4\pi\sqrt{3}n^{1/3}\tilde{\rho}_n)$ and the saturated length, which increase. The maximum harmonic power that can be reached in the independent harmonic generation, $P_{F,n} \approx \sqrt{2}\tilde{\rho}_n P_{beam}$, where $P_{beam} = EI_0$ is the beam power, in turn decreases.

Further corrections come due to the energy spread and emittance and read as follows [45,46]:

$$L_{n,g} = L_{n,g}^0 \kappa \Phi_n, \quad L_s \cong 1.07 L_g \ln \frac{9\eta_1 P_{F,1}}{P_0}, \quad P_{n,F} \cong \sqrt{2} \frac{\eta_n \tilde{\rho}_n P_{beam}}{\kappa}, \quad (10)$$

where the phenomenological coefficients are [25–36]:

$$\begin{aligned} \Phi_n &\cong \left(\nu \sqrt{n} + 0.165 \mu_{e,n}^2 \right) e^{0.034 \mu_{e,n}^2}, \quad \mu_{e,n} \cong \frac{2\sigma_\epsilon}{n^{1/3} \tilde{\rho}_n}, \quad \eta_n \\ &\cong 0.942 \left(e^{-\Phi_n(\Phi_n - 0.9)} + \frac{1.57(\Phi_n - 0.9)}{\Phi_n^3} \right) \end{aligned} \quad (11)$$

and ζ describes the effect of the emittance and it is usually close to unity, $\zeta \cong 1 - 1.03$, for a matched beam; its expression is cumbersome [46] and we omit it for brevity. The effect of ζ on the second and third harmonics is minor, but for a beam with large emittance there may be $\zeta \approx 1.1 - 1.4$. In this case the convolution (7) is needed instead of (6) for the spontaneous UR. The details are available in our preceding publications [31–38]. In their nonlinear generation, the harmonic powers are induced by the fundamental tone and they grow as the n -th power of the fundamental, $\propto e^{nz/L_g}$, which is faster than in their linear independent generation $\propto e^{z/L_{n,g}}$ [4–10,46,49,50]. The evolution of the n -th harmonic in the segmented undulator goes exponentially as a sum of the following linear term $P_{L,n}$ and induced by the fundamental nonlinear term Q_n [53]:

$$\begin{aligned} P_{L,n}(z) &\cong \frac{P_{n,0} S_n(z)}{1 + \left(1.3 P_{n,0} S_n(z) / P_{n,F} \left(1 + 0.3 \cos \left((z - L_s) / 1.3 L_{n,g} \right) \right) \right)}, \\ Q_n(z) &\cong \frac{\tilde{P}_{n,0} e^{nz/L_g}}{1 + (e^{nz/L_g} - 1) \frac{\tilde{P}_{n,0}}{P_{n,F}}} + \frac{P_{n,0} e^{nz/L_g}}{1 + (e^{nz/L_g} - 1) \frac{P_{n,0}}{P_{n,F}}} \end{aligned} \quad (12)$$

where

and [46]:

$$S_n(z) \cong 2 \left| \cosh \frac{z}{L_{n,g}} - e^{\frac{z}{2L_{n,g}}} \cos \left(\frac{\pi}{3} + \frac{\sqrt{3}z}{2L_{n,g}} \right) - e^{-\frac{z}{2L_{n,g}}} \cos \left(\frac{\pi}{3} - \frac{\sqrt{3}z}{2L_{n,g}} \right) \right| \quad (14)$$

The saturation of a FEL harmonic is primarily due to the saturation of the fundamental and the saturated harmonic power reads, for example, as follows [45,46]:

$$P_{n,F} = \frac{\eta_n}{\eta_1} \frac{P_{1,F}}{\sqrt{n}} \left(\frac{f_n}{\eta f_1} \right)^2 \quad (15)$$

From (15) it is evident that the Bessel coefficients $f_{n,x,y}$ must describe all effects and determine the result. For the even harmonics the angular contributions are of paramount importance; they originate from the misalignment of the beam and from the finite size of the beam; moreover, besides the divergence, the effective angle of the photon-electron interactions in the beam section plays important role. Betatron oscillations in narrow relativistic beams contribute little. The validity of formulae (11) - (15) has been verified in [31–38] with known documented data of all major FELs operating in the world.

Several alternative analytical formulations for the FEL harmonic powers in the regime of nonlinear generation were proposed by independent authors. In [51] Huang with co-authors gave simple formula for the third and second harmonic powers P_3 and P_2 , induced by the fundamental power P_1 :

$$\begin{aligned} P_{Huang3} &= \Theta \rho P_{beam} (P_1 / (\rho P_{beam}))^3, \\ P_{Huang2} &= P_n \left(\frac{\lambda_u k f_2}{\gamma 2\pi \sigma_{x,y} f_n} \frac{b_2}{b_n} \right)^2, \quad n = 1 \text{ or } 3, \end{aligned} \quad (16)$$

where the numerical coefficient Θ has the estimated value of $\sim 10^{-1}$ (see [51]). The results of the authors of [51] and our independent estimations both show that (16) yields one order of magnitude higher value for the third harmonic power than the respective measurements. We suggest the phenomenological coefficient $\Theta \approx 0.01$ in (16), which restores the

agreement of the predicted power P_3 with the measured data for many FELs. Formula (16) for P_2 [51] expresses the second harmonic power in terms of the power of the fundamental $n = 1$ or the third harmonics $n = 3$; we rewrite it from [51] as follows:

$$P_{Huang\ 2} = P_n \left(\frac{\lambda_u k f_2 b_2}{2\pi f_n b_n} \right)^2 \frac{\theta^2}{(\gamma \epsilon_{x,y})^2}, \quad n = 1 \text{ or } 3, \quad (17)$$

where the beam section $\sigma_{x,y}$ and the bunching coefficients for second harmonic b_2 and for the harmonics $n = 1$ or 3 are involved. The estimate for second harmonic power P_2 varies in the range of one order of magnitude, dependently on the choice of $n = 1$ or $n = 3$ for the referent harmonic. We distinguished in the r.h.s of formula (16) for P_2 the off-axis angular dependence θ , so that the original result of Huang (16) for P_2 [51] appears upon the assumption of the divergence angles for θ in our form (17). We remind that the relation between the beam cross section Σ , emittances $\epsilon_{x,y}$, divergences $\theta_{x,y}$ and beam sections $\sigma_{x,y}$ is the following:

$$\Sigma = 2\pi\sigma_x\sigma_y, \quad \sigma_{x,y} = \sqrt{\epsilon_{x,y}\beta_{x,y}} = \epsilon_{x,y}/\theta_{x,y}, \quad \beta_{x,y} = \epsilon_{x,y}/\theta_{x,y}^2. \quad (18)$$

In most cases formula for the second harmonic power P_2 in its original form (16) predicts lower than measured power. To describe experiments correctly we must account for the recently discovered in [31–38] effect of the angle of the electron-photon interaction $\bar{\theta} = \sigma_\gamma/L_g$, where σ_γ is the photon beam section, and account for it instead of the divergences in (17); then we get correct estimation. Another formula for the second harmonic power P_2 was proposed by Gelsoni and co-authors in [52]: P_2 reads in terms of the fundamental power P_1 with account for the Fresnel number $\Gamma = \Sigma/L_u\lambda_1$. The latter describes difference in the phases of the waves, coming from the centre and from the edges of the beam of the cross section Σ to the undulator end, distant at the section length L_u . We reformulate the author’s formula [52], explicitly distinguishing the terms as follows:

$$P_{Gelsoni\ 2} \cong P_1 \frac{\Delta}{\Gamma}, \quad \Delta = \frac{(2K(J_0(K) - J_2(K)) + J_1(K))^2 + (J_1(K))^2}{(24\pi)^2 K(J_0(K/2) - J_1(K/2))^2}, \quad (19)$$

where $J_{0,1,2}(K)$ [52] are the Bessel functions of the argument $K = k^2/\left(2\left(1 + k^2/2\right)\right)$, not related to the Bessel coefficients $f_{n,x,y}$, which describe the normalized amplitudes of the UR harmonics.

Further analysis of different analytical formalisms for the FEL harmonic powers will be done elsewhere. In what follows we will use proven reliable formulation (11)–(15) to analyze the effect of the variation of main beam parameters on the harmonic radiation.

3. Modelling radiation at SPARC FEL

In this section we consider the radiation from SPARC undulators in the visible range $\lambda_1 \sim 500$ nm [19,27]. Some data for the beam and undulators of SPARC is collected in Table 1.

Table 1
Parameters of the beam and undulators of SPARC [19].

Electron beam				Undulator section	
parameter	value	parameter	value	parameter	value
I_0 , A	53	σ_e , %	0.05–0.1	λ_u , cm	2.8
E_e , MeV	152	β_x , m	1.5	L_u , m	2.1
$\gamma\epsilon_{x,z}$, m × rad	2.9×10^{-6}	β_y , m	1.5	N	75
$\gamma\epsilon_{y,z}$, m × rad	2.5×10^{-6}	radius, μm	120	k	2.07
				number of sections	6

3.1. The spontaneous UR analysis for SPARC undulators

In this section we discuss the parameters of the installation as reported for the experiment in [19] and their effect on the spontaneous radiation spectrum of SPARC undulators as well as the influence of the variation of the energy spread and of the emittance on the spontaneous harmonic radiation; to this end we model analytically and numerically the spontaneous UR at SPARC installation.

The intensities of harmonics of the spontaneous UR of SPARC are shown in Fig. 1. The spectrum is typical for a planar undulator; it consists of strong odd and weak even harmonics. The beam has rather small absolute emittance $\epsilon_{x,y} \sim 9 \times 10^{-9}$ m × rad, small divergence $\theta_{div} \approx 0.02$ and low energy spread: $\sigma_e = 0.05\%$ – 0.1% . The deflection parameter of SPARC undulators is quite small, $k = 2$; the third spontaneous UR harmonic is the strongest of all; it is evident in Fig. 1b for the beam with low energy spread $\sigma_e = 0.05\%$. Higher beam energy spread $\sigma_e = 0.1\%$ affects high harmonics rather than the fundamental; for $\sigma_e = 0.1\%$ we see in Fig. 1 the decrease of high harmonic powers as compared with their intensities for $\sigma_e = 0.05\%$. The third UR harmonic is as strong as the fundamental for higher energy spread $\sigma_e = 0.1\%$ (see Fig. 1a) and higher harmonics in general are noticeably weaker in this case (compare Fig. 1a, b). The decrease of the energy spread below $\sigma_e = 0.05\%$ has fairly weak effect on the intensity of the harmonics at SPARC. The result of the comprehensive analytical account for the emittance and energy spread in the convolution (7) does not noticeably differ from the simpler evaluations with (6), where only the energy spread effect is considered; we omit proper plots for brevity. The analytical results agree quite well with our accurate numerical simulations with SPECTRA (compare Fig. 1b with Fig. 1c).

For the spontaneous UR it is rather common that high harmonics intensity reaches and exceeds that of the fundamental tone. Among the losses, which affect the harmonic intensities, main role plays the energy spread as can be seen upon the comparison of Fig. 1a vs Fig. 1b. The energy spread in Fig. 1 b is rather low and then the third harmonic is the strongest and the fifth is as strong as the fundamental in the spontaneous radiation spectrum. Accurate numerical simulation with specialized SPECTRA software accounts for all losses; thenumerical results in Fig. 1c confirm our analytical evaluation, shown in Fig. 1b. For higher values of the undulator deflection parameter k , the maximum of the harmonic intensity shifts towards higher harmonics, so that for wigglers with $k \sim 7$ – 10 , the spectrum may contain a hundred of strong harmonics, in a way similar to the spectrum of a magnetic chicane or of a bending magnet. While this is common for the spontaneous radiation, it is not true for the stimulated radiation in modern electron cyclotron masers and free electron lasers. In these devices high harmonics are usually much weaker than the fundamental due to weaker bunching at their wavelengths and the saturation of the fundamental limits growth of the harmonic powers (in what follows the example of the bunching evolution in LEUTL FEL is shown in Fig. 6 b).

3.2. Modelling and analysis of the FEL radiation at SPARC

Here we model and discuss the reported radiation of FEL harmonics in the experiments at SPARC and the effect of variation of the energy spread and emittance of the beam on the harmonic radiation. In SPARC experiments only the fundamental and the third harmonics were detected [19,27]. The maximum collected pulse energy at SPARC was $E_\gamma \approx 0.01$ mJ; the energy measurement was made after the sixth undulator and it was said to be close to saturation. From the reported electron bunch length $\tau_e \approx 2.5$ ps we estimate the photon pulse duration: $\tau_\gamma \cong \sqrt{2\pi\tau_e} \sqrt{L_g/L_s} \approx 1.5$ ps. The respective power for the maximum pulse energy is ~ 7 MW and it matches the maximum of the measured power range at 12.5 m. The evolution of FEL harmonic powers along pure undulator length is shown in Fig. 2. The SPARC FEL has six undulator sections of the total length ~ 12.5 m. It was reported that the

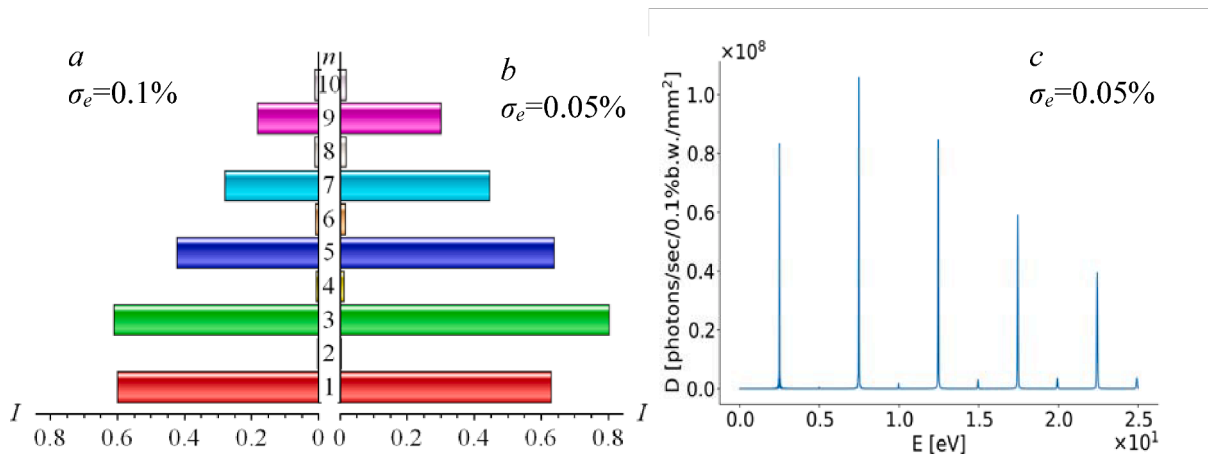


Fig. 1. SPARC spontaneous UR spectrum a) analytical result for energy spread $\sigma_e = 0.1\%$, b) analytical result for energy spread $\sigma_e = 0.05\%$, c) numerical result of SPECTRA for energy spread $\sigma_e = 0.05\%$.

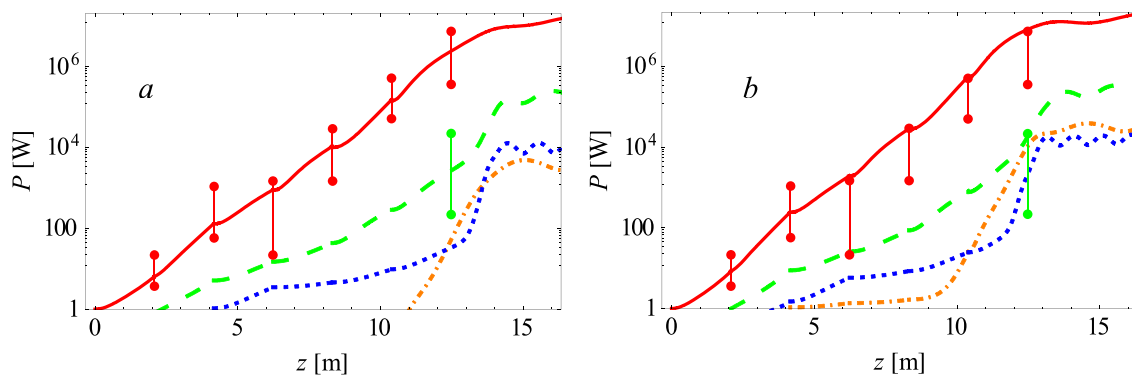


Fig. 2. SPARC FEL harmonic power evolution along undulators, $\gamma\varepsilon = 2.7 \mu\text{rad} \times \text{m}$, energy spread: a) $\sigma_e = 0.1\%$, b) $\sigma_e = 0.05\%$. Harmonics are denoted by coloured lines: $n = 1$ — red solid, $n = 2$ — orange dashdotted, $n = 3$ — green dashed, $n = 5$ — blue dotted, connected coloured dots denote experimentally measured data range. (For interpretation of the references to colour in this figure legend, the reader is referred to the web version of this article.)

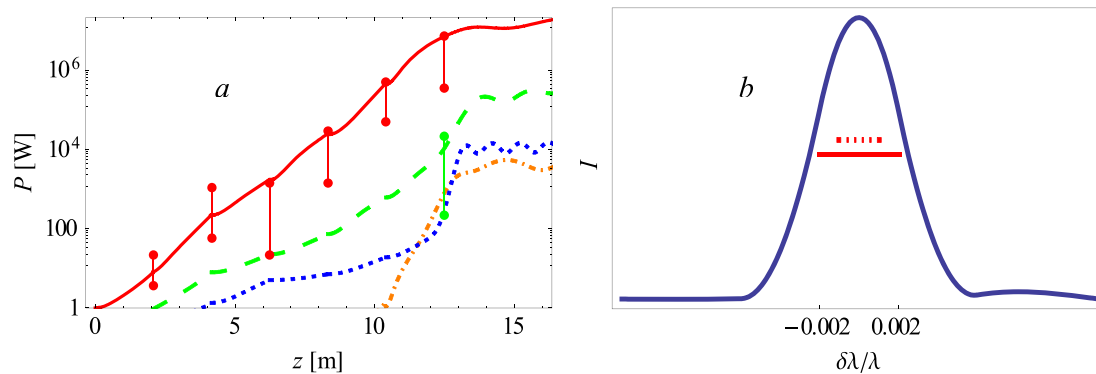


Fig. 3. A) SPARC FEL harmonic power evolution along undulators, $\gamma\varepsilon = 2.0 \mu\text{rad} \times \text{m}$, energy spread $\sigma_e = 0.1\%$. Harmonics are denoted by coloured lines: $n = 1$ — red solid, $n = 2$ — orange dashdotted, $n = 3$ — green dashed, $n = 5$ — blue dotted, coloured dots denote experimentally measured data range. b) — radiation spectral density; calculated — blue line, measured — red line, SASE estimate — red dotted line. (For interpretation of the references to colour in this figure legend, the reader is referred to the web version of this article.)

saturation was not achieved at the end of the last undulator section at SPARC installation. We extended our analysis beyond the total length of the six undulators to study the saturation domain and the respective saturated harmonic powers for various beam parameters. Our theoretical predictions for the harmonic powers are denoted by the colored lines in Fig. 2a,b and Fig. 3a: $n = 1$ — red solid, $n = 2$ — orange dashdotted, $n = 3$ — green dashed, $n = 5$ — blue dotted lines, the colored

dots denote the measured values range. We compared our results with those reported after each undulator section and we model the FEL saturation region, which would be in the upstream undulators beyond the actual undulators installed at SPARC. Our theoretically predicted power for the fundamental is denoted by the red solid line and it exactly matches the highest experimental values along the FEL if we assume the default emittance $\varepsilon_{x,y} \approx 2.7 \text{ mm} \times \text{mrad}$ and the lowest reported energy

spread $\sigma_e = 0.05\%$ (see Fig. 2b). For larger spread, the fundamental FEL power is expectedly lower; it remains in the measured range close to the average values (see Fig. 2a). The calculated gain length is $L_g \approx 0.6$ m; the saturation is expected after $L_g \approx 13$ –14 m of pure undulator length.

We have analyzed possible FEL harmonic power evolution for the whole range of variation of the beam parameters all along and beyond the length of the six undulator sections in the saturation domain. Following the suppositions in [19] that the emittance was possibly smaller than that measured, we assumed its value $\gamma\epsilon_{x,y} = 2.3$ mm \times mrad and assumed slightly larger Twiss parameter $\beta = 1.6$ m to keep the beam section invariant; then we got the harmonic power evolution practically identical that in Fig. 2b, where the standard setup is assumed; the computed power is at the upper limit of measured range; the value of the energy spread was kept invariant $\sigma_e = 0.05\%$. Moreover, as suggested by reports in [19], we assumed even smaller emittance $\gamma\epsilon_{x,y} = 2.0$ mm \times mrad and for some higher energy spread $\sigma_e = 0.1\%$ we got for the harmonic powers (see Fig. 3a) very close to their values in the case of the default emittance $\gamma\epsilon_{x,y} = 2.7$ mm \times mrad and lower energy spread $\sigma_e = 0.05\%$. They were at the upper range of the experimental values, as shown in Fig. 3a. Thus the evolution of the fundamental FEL power in the assumption of the higher beam emittance, $\gamma\epsilon_{x,y} = 2.7$ mm \times mrad, and lower energy spread, $\sigma_e = 0.05\%$, is same as the evolution of the fundamental for lower emittance, 2.0 mm \times mrad, and higher energy spread, 0.1%; all the values are in the measured range (compare Fig. 3a vs Fig. 2b). The reason for such behaviour is in the higher current density for smaller beam emittance, which shortens the gain length; this effect is counteracted by larger electron energy spread, which extends the gain so that the resulting FEL gain barely changes. Our analysis confirms the suppositions of the authors of the experiment in [19], that real values of the installation may be somewhat different from those measured in the studied range. Nevertheless, the results are within the range of the experimental values.

Let us discuss the influence of the angle of the photon-electron interactions on the harmonic radiation. For the stimulated UR in general, high FEL harmonics generally are suppressed contrary to the spontaneous UR harmonics; FEL harmonics extinguish rapidly with increase of the harmonic number n since bunching at the high harmonic wavelength is very sensitive to all kind of losses, such as the energy spread, the divergence etc. However, there can be five harmonics in SPARC FEL spectrum; the fifth harmonic is allowed by both conditions: $\epsilon_{x,y} \sim \lambda_s/4\pi$ and $\sigma_e \approx \rho_5$. Several numerical programs were used by the authors of SPARC FEL experiment [19] and by other researchers [27]. The numerical results from different from each other codes for simulation of the FEL have the discrepancy of one order of magnitude for the fundamental and two orders of magnitude for the third harmonic. Our analytical results for the harmonic powers are obtained with account not only for the beam diffraction, energy spread and emittance, but also for the effective angle of the photon-electron interactions, $\gamma\bar{\theta} \approx 0.06$, in the beam on one gain length; this angle is three times the divergence angle, $\theta_{div} \gamma \approx 0.02$. Then we get the resulting harmonic powers at the highest measured values for the best FEL performance and they are within the range of discrepancy of results of the numerical simulations in [19,27]. If we ignore the effective angle of the photon-electron interactions, then we get way too low second harmonic power. The calculated values for the gain L_g , saturation length L_s , and FEL amplification factor $\sim 10^7$, match the experimental data. For the reported pulse energy $E_p \approx 0.01$ mJ we calculated the saturated FEL harmonic content for the second harmonic: $\sim 0.15\%$, for the third harmonic: $\sim 1\%$, and for the fifth harmonic: $\sim 0.1\%$, in good agreement with the available data.

We also estimated the FEL harmonic saturated powers, following two alternative theoretical approaches. Original formula (16) by Huang (see [51]) predicts the third harmonic power P_3 higher by an order of magnitude than that measured. With our phenomenological correction coefficient $\Theta \approx 10^{-2}$, we estimate the third harmonic power $P_3 \sim 0.25$ MW in agreement with the measurements. For the second harmonic, the

approach [51] yields too low power. Instead of the divergence, originally supposed in (16) and (17) for the angle θ , we assume the effective angle of electron-photon interaction $\bar{\theta}$ in (17) since this angle is the largest of all other angular contribution and it yields correct prediction in our model (11)–(15). With account for $\bar{\theta}$, the formalism of Huang also yields reasonable power range for the second harmonic: $P_2 \sim 10$ –80 kW, which is determined by the values $P_{1,3}$ and agrees with our theoretical result $P_2 \sim 30$ kW from (11)–(15). Following the alternative approach of other authors in [52], we get very high predicted second harmonic power from (19); it appears almost as high as the third harmonic power, $P_3 \sim 0.15$ MW as detected at SPARC; this value for the second harmonic seems unrealistic because of the second harmonic was not detected in SPARC experiments at all and also because of the emittance was quite low in the fairly narrow electron beam of SPARC; so there were no obvious reasons for abnormally strong second harmonic at SPARC.

The radiation spectral line was measured between 496 and 498 nm [19], which yields the radiation spectral density $\sim 0.4\%$ [19]; it is shown by the red solid line in Fig. 3b. Our analytical estimation of the spectral width involves the Bessel coefficients (3) and the result denoted by the blue line in Fig. 3b agrees with the experiment. The general estimate for SASE yields smaller value: $\Delta\lambda/\lambda \cong \sqrt{\rho_1/(L_s/\lambda_u)} \approx 0.2\%$; it is shown by the red dotted line in Fig. 3b.

4. LEUTL FEL

We consider the radiation of visible light at the wavelength $\lambda_1 \sim 530$ nm at LEUTL FEL [17,18].

4.1. The spontaneous UR analysis for LEUTL undulators

In this section we discuss the parameters of the installation in comparison with SPARC and their effect on the spontaneous radiation spectrum of LEUTL undulators as well as the influence of the variation of the energy spread and of the emittance on the spontaneous harmonic radiation; to this end we model analytically and numerically the spontaneous UR at LEUTL installation. LEUTL and SPARC have similar each other radiation wavelengths and electron beam energies. However, the beam quality is much better at SPARC also because it was built a decade later than LEUTL. There is a difference between their beams: at LEUTL the beam section, $\sigma_{x,y} = 0.25$ mm, is twice as wide as that at SPARC; the divergence at LEUTL, $\theta_{div} \approx 0.17$ mrad, $\gamma\theta_{div} \approx 0.085$, is four times that at SPARC; the emittance at LEUTL, $\gamma\epsilon_{x,y} \sim 6\pi$ – 9π mm \times mrad, is seven times that at SPARC. The deflection parameter of the LEUTL undulators, $k = 3.1$, is larger than at SPARC, where $k \approx 2.1$. In what follows we model, analyze and compare with each other the radiation in two LEUTL experiments with different from each other emittances and currents and compare with the radiation at SPARC; the harmonics at LEUTL were accurately measured after each undulator section. Some data for the beam and undulator for the two LEUTL experiments [17,18] is given in Table 2.

First consider the LEUTL experiment from August 2001 [18]; in this experiment the emittance, $\epsilon_{x,y} \approx 6\pi$ mm \times mrad, was smaller than in

Table 2
Parameters of the beam and undulator of LEUTL [18].

Electron beam		Undulator section			
parameter	value	parameter	value		
I_0 , A	210 A or 505A	σ_e , %	0.1	λ_u , cm	3.3
E , MeV	217	β_x , m	1.5	L_u , m	2.4
$\gamma\epsilon_x$, m \times rad	$5.9\pi \times 10^{-6}$ or $8.3\pi \times 10^{-6}$	β_y , m	1.5	N	72
$\gamma\epsilon_y$, m \times rad	$6.4\pi \times 10^{-6}$ or $9\pi \times 10^{-6}$	$\sigma_{x,y}$, μm	~ 250	k	3.1
				number of sections	8

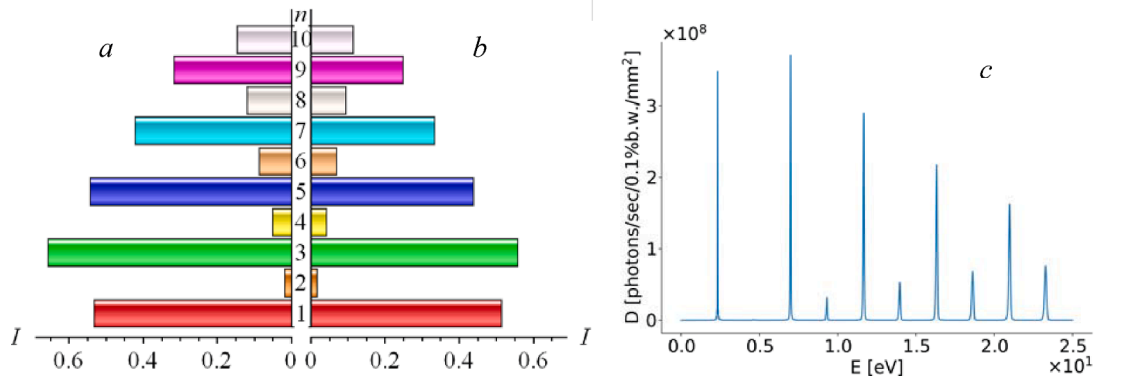


Fig. 4. Theoretical spontaneous UR spectrum for LEUTL, $\gamma\epsilon = 6.2\pi \mu\text{rad} \times m$: a) — analytical with account for the emittance and energy spread in the convolution, b) — analytical with account for the energy spread alone in, c) — numerical with SPECTRA.

earlier experiments at the same installation. The betatron effects in a wide beam may contribute to the harmonic radiation. We have accounted for both betatron oscillations and large emittance as well as for the energy spread and took proper convolution for the spontaneous UR with the Bessel coefficients. We now compare the spectrum with account for the losses computed by (7) with the result of the simple convolution (6), where only the energy spread is accounted for; we also computed the spectrum numerically with the help of SPECTRA program. The result of the comprehensive convolution (7) in Fig. 4a is very close to the numerical result in Fig. 4b; the account for the energy spread alone (6) in yields slightly stronger high harmonics in the spectrum and is omitted for brevity.

Let us explore the contribution of the betatron oscillations to the harmonic intensities and on the radiation line width. It is worth mentioning that even harmonics in LEUTL spectrum are mainly due to the angular effects and not to the betatron oscillations. The Bessel coefficients for the harmonics n read as follows: $f_{n=1,\dots,10} = \{0.753, 0.073, 0.334, 0.077, 0.218, 0.078, 0.158, 0.078, 0.119, 0.076\}$. We distinguished the contributions from the betatron effects and found that they were absolutely negligible for odd harmonics. The betatron contributions to the Bessel factors for the even harmonics read as follows: $f_{n=2,4,6,8,10}^{\text{betatron}} = \{0.019, 0.014, 0.011, 0.009, 0.008\}$. They are not negligible, but they contribute with less than quarter of the total values for the even harmonics and their effect is minor. The radiation line of LEUTL is split into betatron harmonics distant from each other by the wavelength interval $\delta\lambda \cong k\lambda/n\sqrt{2}\gamma|_{n=1} \cong 2.7 \text{ nm}$. For the Bessel functions we get the following values: $\tilde{J}_{p=-3,\dots,+3} = \{0.00, 0.08, 0.47, 0.75, 0.43, 0.16, 0.04\}$ and we see that the harmonics with numbers $p = -1, \dots, 1$ contribute mainly. Thus we end up with the total width of the split line $\Delta \cong 5.5 \text{ nm}$ at

the radiation wavelength $\lambda_1 = 532 \text{ nm}$. The respective spectral density is therefore $\Delta/\lambda \cong 0.01$, which is comparable with the natural width, $0.9/N|_{N=72} = 0.0125$, of the UR line.

Let us discuss the effect of the emittance in itself on the spectrum. Comparing with each other plots in Fig. 4 a vs b, we note that large emittance in itself affects the spontaneous UR at LEUTL. Analytical calculations with account for the energy spread alone yield stronger high harmonics (see Fig. 4a) than those computed with SPECTRA code (see Fig. 4c), where all effects were accounted for numerically. The analytical account for the emittance in the convolution (7) yields the harmonics shown in Fig. 4 b; the proportions of the analytically obtained harmonic intensities are close to those in the numerical SPECTRA result in Fig. 4 c. For even larger beam emittance $\gamma\epsilon_{x,y} \cong 8.5\pi \text{ mm} \times \text{mrad}$ in the other LEUTL experiment [18], the calculated UR spectrum is shown in Fig. 5. Our analytical result accounts for the spectrum degradation due to both the emittance and the energy spread in Fig. 5b. The account for the detrimental effect of energy spread alone yields the result in Fig. 5a. The common degrading effect of the energy spread and large emittance yields weaker high harmonics as shown in Fig. 5b, in comparison with their intensities in Fig. 5a, where only the energy spread was considered. The comprehensive SPECTRA numerical result in Fig. 5c is close to our analytical evaluation (7) (see Fig. 5b) where we accounted for the energy spread and emittance. Note that for the radiation from SPARC undulators we also used both convolutions (6) and (7) and they yielded very close to each other results due to small emittance of the beam at SPARC.

4.2. Modelling and analysis of the FEL radiation at LEUTL

Here we model and discuss the radiation of FEL harmonics in the

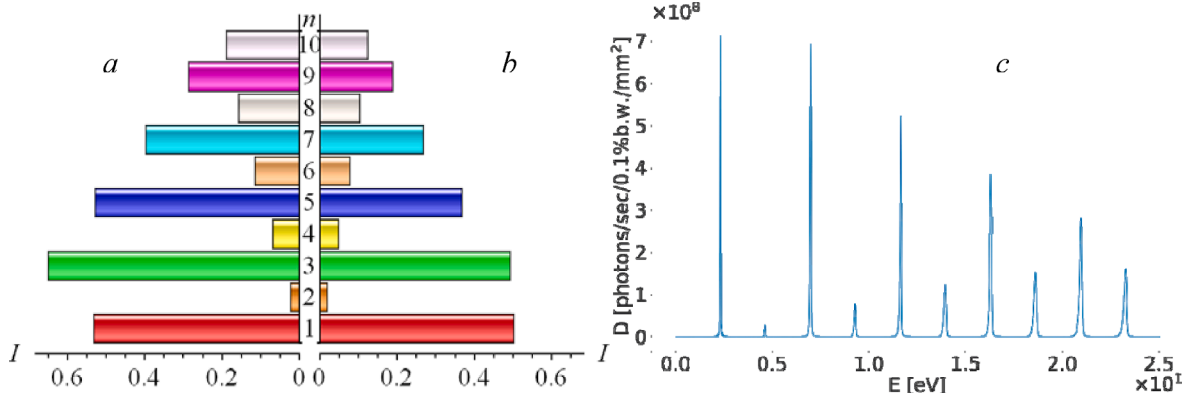


Fig. 5. Theoretical spontaneous UR spectrum for LEUTL, $\gamma\epsilon = 8.5\pi \mu\text{rad} \times m$: a) — analytical with account for the emittance and energy spread in the convolution, b) — analytical with account for the energy spread alone in, c) — numerical with SPECTRA.

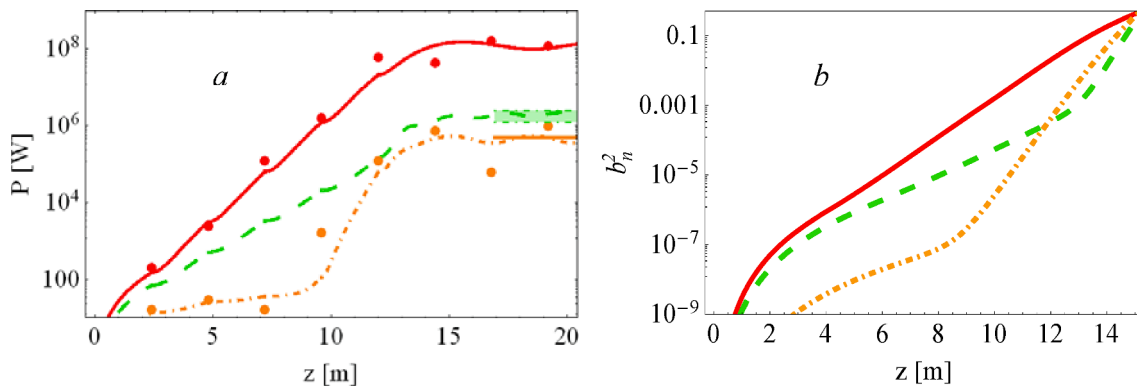


Fig. 6. Modelling of LEUTL experiment from August 2001, $\gamma\varepsilon_{x,y} = 6.2\pi \text{ mm} \times \text{mrad}$, $I_0 = 210\text{A}$, $\lambda_1 = 530 \text{ nm}$; a) harmonic power evolution along undulators, b) harmonic bunching evolution along undulators. Harmonics are denoted by coloured lines: $n = 1$ — red solid, $n = 2$ — orange dot-dashed, $n = 3$ — green dashed; experimental values are shown by the coloured dots; average experimental value $P_2 = P_1/240$ — orange thick line after 16 m. (For interpretation of the references to colour in this figure legend, the reader is referred to the web version of this article.)

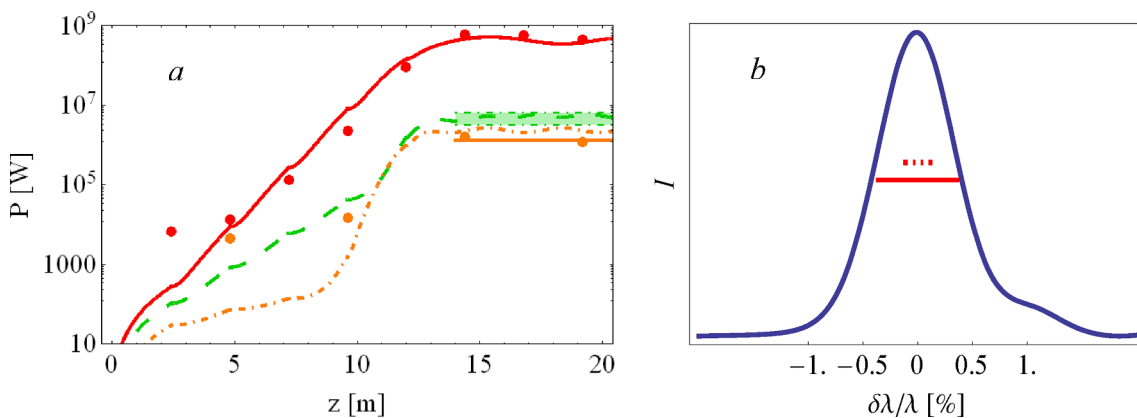


Fig. 7. A) harmonic power evolution along LEUTL undulators in experiment in March 2001, $\lambda_1 = 530 \text{ nm}$, $\gamma\varepsilon_{x,y} = 9\pi \text{ mm} \times \text{mrad}$, $I_0 = 505\text{A}$. Harmonics are denoted by coloured lines: $n = 1$ — red solid, $n = 2$ — orange dot-dashed, $n = 3$ — green dashed; experimental values are shown by the coloured dots; average experimental value $P_2 = P_1/240$ — orange thick line after 16 m; b) the radiation line spectral density: analytically calculated — blue line, measured at half-height — red line, general SASE width estimate — red dotted line. (For interpretation of the references to colour in this figure legend, the reader is referred to the web version of this article.)

experiments at LEUTL and analyze the influence of variation of the energy spread and emittance of the beam on the harmonic radiation as well as that of the electron-photon interaction and of the betatron oscillations in the beam of finite size. Among FEL experiments at LEUTL, we considered two with the most complete radiation measurements (see [18] and some data in Table 2). Main difference in the setup of the experiments was in the beam emittance and current. The conditions $\varepsilon_{x,y} \leq \lambda_0/4\pi$, $\sigma_e \leq \rho/2$ are strictly fulfilled only for the fundamental; for the harmonics $n = 2, 3$, the emittance exceeds $\lambda_{2,3}/4\pi$ and the energy spread is comparable with the Pierce parameter: $\sigma_e \approx \rho_2 \approx 0.7\rho_3$. The first and second harmonics were detected and measured [18] all along the undulators; their reported experimental values along the undulators are shown in Fig. 6a by coloured dots, following [18]. The third harmonic saturated power was 1–2 % of the fundamental (green area after 16 m), the second harmonic average rate was 1/240 in all experiments (solid orange line). Our analytically computed harmonic powers and the bunching values along the undulators are shown by the coloured lines in Fig. 6 a and b respectively. We accounted for the emittance, betatron oscillations and effective angle of the electron-photon interaction in the beam; the latter largely determines even harmonic powers in a FEL; the off-axis deflection was not reported for LEUTL. Our theoretical results for both LEUTL experiments perfectly match the measurements (see Fig. 6a and Fig. 7a). For the second harmonic power, calculated with account for the emittance and betatron oscillations neglecting the

effective angle of the electron-photon interaction, we get much lower theoretical power than that measured [31–35]. We calculated the effective angle of photon-electron interactions: $\bar{\theta} \approx \sigma_{x,y}/L_{\text{gain}} \approx 0.28 \text{ mrad}$, $\gamma\bar{\theta} \approx 0.14$; it is larger than the divergence: $\gamma\theta_{\text{div}} \approx 0.07$. For the second harmonic the contribution from betatron effects compares with that from the angular effects in y-polarization in (3): $f_{n=2,p}^\beta \sim f_{n=2,y} \approx 0.02$. With account for the effective angle of photon-electron interactions $\bar{\theta}$ we get much larger Bessel factors for the second harmonic: $f_{n=2,x} \approx 0.14 \gg f_{n=2,y} \sim f_{n=2,p}^\beta \approx 0.02$, which determine the radiation of the second harmonic. We obtained the gain $L_{\text{gain}} \approx 0.75 \text{ m}$ and saturation length $L_s = 16 \text{ m}$, in agreement with the reports [18].

Note that despite the electron currents in two LEUTL experiments were different from each other, the gain length in both experiments was almost the same. This can be explained by larger emittance in the experiment with higher current. Larger emittance counteracted the effect of higher current by reducing the current density and by itself imposing the losses, so that at the end the gain length did not change significantly. In the early experiment high measured values of the radiation power after the first and second undulators (see Fig. 7a) were explained in [18] by high noise levels and by the fundamental tone, entering the detector of the second harmonic. In the later experiment the setup was improved and more measuring stations were added. The agreement of the theory with the experiment in this case is close to perfect also after the first undulators (see Fig. 6a).

The bunching evolution is shown in Fig. 6b and it corresponds well with the power growth along the undulators in Fig. 6a. The bunching of the third harmonic closely follows that of the fundamental in the linear regime along first 5 m of the undulators, where the powers of the harmonics $n = 1$ (red solid line) and $n = 3$ (green dashed line) are close to each other. The bunching of the third harmonic grows noticeably slower than that of the fundamental and so does the power (compare Fig. 6 a and b). After 13 m, where the green dashed line, denoting the third harmonic in Fig. 6a and Fig. 6b, rises faster, the nonlinear generation of the third harmonic prevails over its independent growth. The harmonic content in saturation was the same in both considered LEUTL experiments; the harmonic evolution in both experiments also looks quite similar in Fig. 6a and Fig. 7a, despite the current and emittance were different; the FEL power was expectedly higher for the higher current in Fig. 7a.

We estimated the third harmonic power with Huang theory [51] applying our correction $\Theta \approx 0.01$ to (16); it yields $\sim 1\%$ content for the third harmonic, which is close to that measured. Estimate for the second harmonic power with the original Huang formula (16) is way too low; however, if we assume in (17) the effective angle of electron-photon interaction $\bar{\theta}$ for the angular contribution θ , then we get $\sim 0.15\%$ content for the second harmonic; it is close to the low measured values for the second harmonic power (see Fig. 6a). The estimation of the second harmonic with by Geloni [52] is in good agreement with the experiment.

The width of the spectral line at LEUTL is determined mainly by the contributions with $p = \{0, \pm 1\}$ in (3), which yield the spectral density $\delta\lambda/\lambda \sim 1\%$ (see Fig. 7b) and agrees with the measurements and reports in [18]; the usual estimate for SASE, $\Delta\lambda/\lambda \cong \sqrt{\rho_1/(L_s/\lambda_u)}$, is significantly smaller (dotted red line in Fig. 7b).

5. SwissFEL

We consider the FEL radiation of hard X-ray light, the wavelength $\lambda_1 \sim 0.1$ nm, in two experiments at the modern SwissFEL facility [54–58], where the radiation is generated by electrons with relatively low for X-ray facility energy, $E = 5.8$ GeV; the LINAC energy spread is low, its absolute value is 350 keV, the designed beam relative energy spread is very low: $\sigma_e = 0.006\%$, the emittances are low: $\gamma\epsilon = 0.4$ mm \times mrad. We consider the radiation at the SwissFEL default wavelength $\lambda_1 = 0.1$ nm in two well documented instances of its operation on two different occasions. In one experiment, the reported energy spread and the emittances were as follows: $\sigma_e = 0.006\%$, $\gamma\epsilon = 0.4$ μm ; the bunch charge was $Q = 0.2$ nC; it produced the photon pulse of the measured duration $\tau_\gamma = 24$ fs, and the collected energy was $E_\gamma = 1$ mJ [54]. The respective electron bunch length was $\tau_e = 40$ fs, the radiation power ~ 40 GW and the computed electron current was $I_0 = 5$ kA. The other FEL experiment [58] followed with lower current, $I = 2$ kA, lower emittance $\epsilon_{x,y} = 0.2$ mm \times mrad [54], but higher energy spread, whose measured value in this experiment was $\sigma_e = 0.0125\%$. Some data on the SwissFEL beam and undulators is collected in Table 3.

Table 3
Parameters of the beam and undulator of SwissFEL.

Electron beam				Undulator	
parameter	value	parameter	value	parameter	value
I_0 , A	2 kA or 5 kA	σ_e , %	0.0125 or 0.006	λ_u , cm	1.5
E , MeV	5800	$\beta_{x,y}$, m	18	L_u , m	4
$\gamma\epsilon_x$, m \times rad	0.2×10^{-6} or 0.4×10^{-6}	β_y , m	18	N	267
$\gamma\epsilon_y$, m \times rad	0.2×10^{-6} or 0.4×10^{-6}	$\sigma_{x,y}$, μm	~ 20	k	1.2
				number of sections	12

The spontaneous UR spectrum from SwissFEL undulators itself is not remarkable; due to the low value of the deflection parameter k and very low losses the fundamental harmonic is dominant in the spectrum; the latter is close to the ideal UR pattern. We omit proper figure for conciseness.

For the FEL radiation at $\lambda = 0.1$ nm we theoretically obtained the saturation length $L_s \sim 30$ m for both considered instances of its operation; it agrees with the measurements. At SwissFEL the saturation length $L_s \approx 30$ m is rather short as compared with most other hard X-ray FELs. For the higher current $I \sim 5$ kA we got some shorter gain $L_g \sim 1.4$ m, for the lower current $I \sim 2$ kA we got longer gain: $L_g \sim 1.7$ m. The harmonic content was similar in both cases. Our analytical modelling of the FEL harmonic powers in SwissFEL is shown in Fig. 8. For the measured radiation pulse energy $E_\gamma = 1$ mJ and the respective pulse time $\tau_\gamma = 24$ fs, proper saturated power is shown by the dashed red line after 25 m in Fig. 8a. The second harmonic content is surprisingly high: $\sim 0.5\%$, higher than that at LCLS for similar radiation wavelength, where the second harmonic content was ~ 0.04 – 0.1% . The beam at SwissFEL is narrow, the emittance is low and the effective angle of the electron-photon interaction is small: $\bar{\theta} \sim 6$ μrad . Low losses at the SwissFEL installation ensured close to ideal conditions for the harmonic radiation from undulators with small deflection parameter k ; the third harmonic content was rather large: $\sim 0.7\%$. However, it is smaller than that at LCLS FEL, where the third harmonic content was $\approx 2\%$ due to high deflection parameter $k = 3.5$ of LCLS undulators.

In one instance of SwissFEL operation, the emittance was two times smaller and the energy spread two times higher, the electron current was 2.5 times weaker than default. The analytical result of the harmonic powers in this case is shown in Fig. 8b. The saturated power was ~ 10 GW, the second harmonic content was $\sim 0.4\%$ and the third harmonic content was $\sim 0.2\%$. Slightly lower content of the third harmonic in this SwissFEL experiment as compared with the other experiment is explained by the higher relative energy spread, which affects high harmonics, even though the energy spread was not really high in any of the SwissFEL experiments.

We calculated the SwissFEL spectral density $\Delta\lambda/\lambda \sim 0.1\%$, within the range $\sim 0.05\%$ – 0.15% , declared by the authors of the experiment in [55]. Computing the Pierce parameter for SwissFEL, we get: $\rho_1 \approx 0.0005$; the estimate for SASE spectral width reads as follows: $\delta\lambda/\lambda \approx \sqrt{\rho\lambda_u/L_s} \approx 0.0005$.

Thus at SwissFEL the increase in the energy spread from the extremely low value 0.006% to the very low value 0.0125% affected high harmonics, which became some weaker, despite the increase of the energy spread was accompanied by the reduction of the emittance by half from $\epsilon_\gamma = 0.4$ $\mu\text{m} \times \text{rad}$ for $\sigma_e = 0.006\%$ to $\epsilon_\gamma = 0.2$ $\mu\text{m} \times \text{rad}$ for $\sigma_e = 0.0125\%$. The reduction of the emittance yields higher current density for the same electron current; this allowed weaker beam current, $I = 2$ kA, for the beam with lower emittance to get the same as in the other experiment gain and saturation length.

6. Conclusions

We have analysed the effect of the beam parameters, such as the emittance, energy spread, current etc. on the harmonic radiation in single pass FELs. With the help of the analytical formalism of generalized forms of Bessel and Airy functions we accounted for the key factors, affecting the harmonic radiation. We also showed that large emittance itself can deteriorate radiation of harmonics. At LEUTL, where the normalized emittance was up to $\gamma\epsilon \approx 9\pi$, its effect was evident for both spontaneous and stimulated radiation. Large emittance caused strong even harmonics of the UR and broadening and distortion of the line shape from the symmetric *sinc* function to the asymmetric Airy-type function shape, accounted by the proper convolution. The harmonic intensity was lower than that computed with common convolution with the energy spread alone by roughly ~ 30 – 40% . For small beam

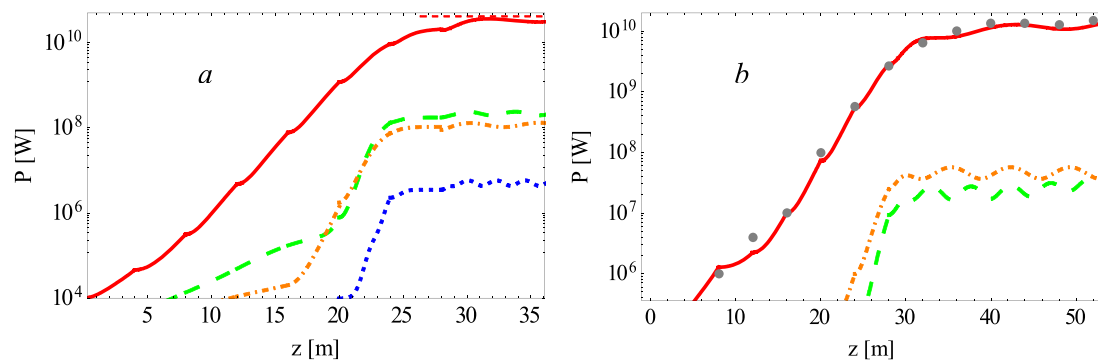


Fig. 8. The harmonic power evolution along the undulators in SwissFEL, $\lambda_1 = 0.1$ nm. The harmonics are denoted by coloured lines: $n = 1$ — red solid, $n = 2$ — orange dashdotted, $n = 3$ — green dashed. a) FEL with the current $I_0 = 5$ kA, emittance $\gamma\epsilon = 0.4$ μm , energy spread $\sigma_e = 0.006$ %, dashed red line denoted saturated power for the collected pulse energy $E_p = 1$ mJ. b) FEL with the current $I_0 = 2$ kA, emittance $\gamma\epsilon = 0.2$ μm , energy spread $\sigma_e = 0.0125$ %, experimental data is shown by dots for the fundamental. (For interpretation of the references to colour in this figure legend, the reader is referred to the web version of this article.)

emittances, such as at SPARC, LCLS, PAL X-FEL, SwissFEL et al., the distortion of the line due to the emittance is irrelevant.

Comparing the FEL radiation in experiments with different beam parameters at the same installations, we found that even harmonics in FELs are determined mainly by the angular effects. We have verified that the second harmonic power is determined mainly by the effective angle of the electron-photon interaction in the beam on one gain length. The emittance itself somewhat reduces the harmonic powers, although the effect is noticeable for high emittance only. However, the beam emittance is related to the beam section and thus the reduction of emittance increases the current density. This in turn increases the gain and the harmonic powers. The energy spread expectedly reduces the harmonic powers and thus counteracts the decrease of the emittance. This was observed, for example, in SwissFEL in two different setups in different experiments.

At LEUTL quite high content of the second harmonic ~ 0.5 % was registered due to large angles of electron-photon interaction. Large emittance on the contrary reduced the harmonic powers, especially for high harmonics. The betatron oscillations were shown to have little effect on even FEL harmonic powers and no effect on odd FEL harmonic powers. The increase of the current and simultaneous increase of the beam emittance in some experiments did not make the gain and saturation shorter, but increased the FEL power. The ratio of the harmonics remained unaffected.

At SPARC, the emittance and energy spread were rather low. Much weaker current than in LEUTL was needed for SPARC to produce similar to LEUTL radiation. The third harmonic was detected at SPARC; its content was ~ 1 %. The betatron oscillations were shown to have no effect on FEL harmonic powers. Variation of the electron energy spread in the range $\sigma_e = 0.05$ – 0.1 % somewhat influences the FEL gain and noticeably changes the second harmonic power. High harmonics become some weaker with the energy spread increase.

At SwissFEL, in one experiment the current and emittance were two times lower and at the same time the energy spread was two times higher as compared with another experiment at the same installation. The saturation length was the same in these experiments and the gain was slightly shorter when the current was two times higher, this also increased the FEL power by four times. Similar effect was observed at LEUTL. The harmonic content of SwissFEL was noticeable due to very low emittance and energy spread; the effect of the increased emittance was compensated by higher current and lower energy spread and vice versa (see details in the text).

The theoretical power estimates from Huang et al. [51] are generally too high for the third harmonic and too low for the second harmonic. The estimates from Geloni et al. [52] are reasonable for even harmonics at LEUTL and SwissFEL, but for SPARC the second harmonic estimate is abnormally high, while it has not been detected in experiments at all.

For both theories the correction consists in that the effective angle of the electron-photon interaction in the FEL must be taken into account; usually it is the largest angular contribution.

The study can be used to evaluate the effect of beam parameters on the performance of other FELs, both operating and under construction.

The authors are grateful to the Referees and Editor for useful notes and advice.

One of the authors, K.Zhukovsky, acknowledges support from the Russian Ministry of Science and Education under grant No. 075-15-2021-1353. Another author, I.Fedorov, acknowledges support from the Foundation for the Advancement of Theoretical Physics and Mathematics Basis, application # 22-2-2-45-1 Stipend Physics Faculty Ph.D Student

Declaration of Competing Interest

The authors declare that they have no known competing financial interests or personal relationships that could have appeared to influence the work reported in this paper.

Data availability

No data was used for the research described in the article.

References

- [1] H. Motz, W. Thon, R.N.J. Whitehurst, *Appl. Phys.* 24 (1953) 826.
- [2] V.L. Ginzburg, On the radiation of microradiowaves and their absorption in the air, *Isvestia Akademii Nauk SSSR (Fizika)* 11 (N2) (1947) 1651.
- [3] J.M. Madey, *J. Appl. Phys.* 42 (1971) 1906.
- [4] B.W.J. McNeil, N.R. Thompson, *Nat. Photon.* 4 (2010) 814.
- [5] C. Pellegrini, A. Marinelli, S. Reiche, *Rev. Mod. Phys.* 88 (2016), 015006.
- [6] P. Schmitser, M. Dohlus, J. Rossbach, C. Behrens, *Free-Electron Lasers in the Ultraviolet and X-Ray Regime*, in: Springer Tracts in Modern Physics, 258, Cham (ZG), Springer International Publishing, 2014.
- [7] Z. Huang, K.J. Kim, *Phys. Rev. ST-AB* 10 (2007), 034801.
- [8] G. Margaritondo, P.R. Ribic, *J. Synchrotron Rad.* 18 (2011) 101.
- [9] E.L. Saldin, E.A. Schneidmiller, M.V. Yurkov, *The Physics of Free Electron Lasers*, Springer-Verlag, Berlin Heidelberg, 2000.
- [10] R. Bonifacio, C. Pellegrini, L. Narducci, *Opt. Comm.* 50 (1984) 373.
- [11] G. Margaritondo, *Rivista del Nuovo Cimento* 40 (9) (2017) 411.
- [12] V.G. Bagrov, G.S. Bisnovaty-Kogan, V.A. Bordovitsyn, A.V. Borisov, O.F. Dorofeev, Ya. Epp V, Y.L. Pivovarov, O.V. Shorokhov, V.C. Zhukovsky, *Synchrotron Radiation Theory and Its Development*, in: V.A. Bordovitsyn, Word Scientific, Singapore, 1999, p 447.
- [13] I.M. Ternov, V.V. Mikhailin, V.R. Khalilov, *Synchrotron radiation and its applications*, CRC Press, 1985.
- [14] G. Margaritondo, *Characteristics and Properties of Synchrotron Radiation*, in: S. Mobilio, F. Boschneri, C. Meneghini (Eds.), *Synchrotron Radiation*, Springer, Berlin, Heidelberg, 2015.
- [15] P. Emma, R. Akre, J. Arthur, et al., *Nat. Photonics* 4 (2010) 641.
- [16] D. Ratner, A. Brachmann, F.J. Decker, et al., *PhysRev ST-AB* 14 (2011), 060701.
- [17] S.V. Milton, E. Gluskin, N.D. Arnold, et al., *Science* 292 (2001) 2037.
- [18] S.G. Biedron, et al., *Nucl. Instrum. Meth. A.* 483 (2002) 94.

- [19] L. Giannessi, D. Alesini, P. Antici, et al., *Phys. Rev. ST-AB* 14 (2011), 060712.
- [20] J.R. Henderson, L.T. Campbell, H.P. Freund, B.W.J. McNeil, *New J. Phys.* 18 (2016), 062003.
- [21] H.P. Freund, P.J.M. van der Slot, D.L.A.G. Grimminck, I.D. Setija, P. Falgari, *New J. Phys.* 19 (2017), 023020.
- [22] H.P. Freund, P.J.M. van der Slot, *New J. Phys.* 20 (2018), 073017.
- [23] K. Zhukovsky, A. Kalitenko, *J. Synchrotron Rad.* 26 (2019) 605.
- [24] K. Zhukovsky, *J. Optics* 20 (9) (2018), 095003.
- [25] K. Zhukovsky, *Results Phys.* 13 (2019), 102248.
- [26] K.V. Zhukovsky, *J. Synchrotron Rad.* 26 (2019) 1481.
- [27] H.P. Freund, P.J.M. van der Slot, *J. Phys. Commun.* 5 (2021), 085011.
- [28] I. Fedorov, K. Zhukovsky, *JETP* 135 (2) (2022) 158–172, <https://doi.org/10.1134/S1063776122080027>.
- [29] K. Zhukovsky, A. Kalitenko, Harmonic generation in planar undulators in single-pass free electron lasers, *Russ. Phys. J.* 62 (2) (2019) 354–362.
- [30] A.M. Kalitenko, K.V. Zhukovskii, *J. Exp. Theor. Phys.* 130 (3) (2020) 327–337.
- [31] K.V. Zhukovsky, *Phys. Uspekhi* 64 (2021) 304.
- [32] K. Zhukovsky, *Opt. Laser Technol.* 131 (2020), 106311.
- [33] K. Zhukovsky, *Eur. Phys. J. Plus.* 136 (2021) 714.
- [34] K. Zhukovsky, *Ann. Phys.* 533 (11) (2021) 2100091.
- [35] K. Zhukovsky, *Rad. Phys. Chem.* 189 (2021), 109698.
- [36] K. Zhukovsky, *Results Phys.* 19 (2020), 103361.
- [37] K. Zhukovsky, *Opt. Laser Technol.* 143 (2021), 107296.
- [38] K. Zhukovsky, I. Fedorov, *Symmetry* 13 (2021) 135.
- [39] B. Prakash, V. Huse, M. Gehlot, G. Mishra, *Optik* 127 (2016) 1639.
- [40] K. Zhukovsky, Analytical account for a planar undulator performance in a constant magnetic field, *J. Electromagn. Waves Appl.* 28 (15) (2014) 1869–1887.
- [41] K.V. Zhukovsky, Harmonic Generation by Ultrarelativistic Electrons in a Planar Undulator and the Emission-Line Broadening, *J. Electromagn. Waves Appl.* 29 (1) (2015) 132–142.
- [42] G. Dattoli, V.V. Mikhailin, K. Zhukovsky, Undulator radiation in a periodic magnetic field with a constant component, *J. Appl. Phys.* 104 (2008), 124507.
- [43] G. Dattoli, V.V. Mikhailin, K.V. Zhukovsky, *Mosc. Univ. Phys. Bull.* 64 (5) (2009) 507–512.
- [44] K.V. Zhukovsky, Operational solution for some types of second order differential equations and for relevant physical problems, *J. Math. Anal. Appl.* 446 (2017) 628–647.
- [45] G. Dattoli, P.L. Ottaviani, S. Pagnutti, *J. Appl. Phys.* 97 (2005), 113102.
- [46] G. Dattoli, L. Giannessi, P.L. Ottaviani, C. Ronsivalle, *J. Appl. Phys.* 95 (2004) 3206–3210.
- [47] M. Xie, *Nucl. Instrum. Meth. A.* 445 (2000) 59.
- [48] M. Xie, in: *Proceedings of the 1995 Particle Accelerator Conference*, IEEE, Piscataway, NJ, 1995, p. 183.
- [49] L. Giannessi, Seeding and Harmonic Generation in Free-Electron Lasers, in: E. J. Jaeschke (Ed.), *Synchrotron Light Sources and Free-Electron Lasers*, Springer International Publishing Switzerland, 2016, https://doi.org/10.1007/978-3-319-14394-1_3.
- [50] R. Bonifacio, L. De Salvo, P. Pierini, *Nucl. Instrum. Meth. A.* 293 (1990) P. 627.
- [51] Z. Huang, K.-J. Kim, *Nucl. Instrum. Meth. A.* 475 (2001) 112.
- [52] G. Geloni, E. Saldin, E. Schneidmiller, M. Yurkov, *Opt. Comm.* 271 (2007) 207.
- [53] K.V. Zhukovsky, *Mosc. Univ. Phys. Bull.* 74 (5) (2019) 480.
- [54] C.J. Milne, et al., *SwissFEL: The Swiss X-ray Free Electron Laser*, *Appl. Sci.* 7 (2017) 720.
- [55] R. Abela, et al., Perspective: Opportunities for ultrafast science at SwissFEL, *Struct. Dyn.* 4 (2017), 061602.
- [56] P. Juranic, et al., *SwissFEL Aramis beamline photon diagnostics*, Erratum, *J. Synchrotron Rad.* 26 (2019) 906.
- [57] R. Abela, et al., The SwissFEL soft X-ray free-electron laser beamline: Athos, *J. Synchrotron Rad.* 26 (2019) 1073.
- [58] E. Prat, et al., A compact and cost-effective hard X-ray free-electron laser driven by a high-brightness and low-energy electron beam, *Nat. Photonics* 14 (2020) 748–754.